HYDROLOGICAL STUDIES OF SELECTED WADIS, ASWAN GOVERNORATE, EGYPT

Sawsan M.M. Ibrahem[1*], Nahla A. Morad[1] and Nemaat A. Youssef[2]
[1]Department of Hydrology, Desert Research Center, Cairo, Egypt
[2]Department of Geology, Desert Research Center, Cairo, Egypt
[*]E-mail: sawsanmoselhy@yahoo.com

Two storms, (November 2021 and August 2024) caused great damage in Aswan City, were selected to investigate the relation between rainfall and runoff. Four Wadis were selected: Abu Aggag, El Heta, Kimb and Umm Boirat. The morphometric analysis revealed that these Wadis have elongated shapes, long time of concentration, which means they can effectively recharge groundwater. During the rainfall event in November 2021, which recorded 18.78 mm of rain over 5 hours, Wadi Abu Aggag received peak flow rates of 119.8 $m^3 s^{-1}$ and a total runoff volume of 3.2 million m^3. The unexpected storm of August 2024, with rainfall depth of 69.72 mm and duration of 46 hours produced a huge amount of runoff water 15.6 million m^3, with maximum flow (515.8 $m^3 s^{-1}$) in Wadi Abu Aggag. This storm is considered as one of the phenomena of climate change in Egypt. The study recommended the construction of detention dams in the up-streams of Wadis El Heta, Kimb and Umm Boirat to delay water flow and enable gradual infiltrate to the groundwater. In addition, constructing a storage dam in the outlet of Wadi Abu Aggag to protect the urban areas from the occasional risk of flash floods and replenishment of the shallow aquifer in the area.

Keywords: hydrograph, storm, morphometric characteristics, rainfall

INTRODUCTION

Forecasting flash floods in drainage basins is particularly challenging, especially in arid areas that lack proper gauging tools. Intense rainfall can have serious effects on hydrologic systems and communities, particularly in arid regions. When rainwater runs off urban surfaces that can't absorb it, it can lead to flooding, significant injuries and traffic disruptions.

Understanding how rainfall relates to runoff is crucial for managing water resources and control flood risk of these areas. Typically, flash floods occur due to heavy rain in arid and semi-arid regions. They are driven by two main types of factors: the first involves changing weather conditions, which vary in space and time and are often underreported because of the limited number of weather stations. The second involves more stable factors, like the ground surface physical and geological characteristics (Youssef et al., 2009).

In Egypt, many areas suffer from the effect of floods which effect on the urban areas. According to Morad et al. (2020), in Wadi El-Halazouni-New Cairo, urban areas play an important role in increasing the volume of runoff from 15.7% in 1984 to 25.91% in 2018, due to the increase in buildings and settlements. The increase of the urban runoff is due to the reduction of the drainage network and increasing of the impervious ratio. In other words, more urbanization results in more runoff.

Saber et al. (2017) discussed the impact of flash floods on Wadi systems in Aswan area and concluded that the constructed urban regions in Aswan cities are constructed without any governmental preplanning, which may lead to the failure and damage of houses, due to the occurrence of any extreme flash floods. Also, the increase in agricultural development and urbanization resulted in great variation of spatial impacts of flash floods where it affected both Wadi residences and urban areas alike.

Recently, Aswan has been subjected to several continuous flash floods, due to extreme rainfall events that caused severe damage to life, vital infrastructures and buildings. The storm of 12 November 2021 in Aswan governorate, many community infrastructures, including more than 1,157 households were affected as several houses were destroyed or partially damaged. While 4,685 people (937 families) were still living in their houses that had been partially damaged and refused to leave. Following the detailed assessment conducted by the Egyptian Red Crescent in November 2021, at least 3 deaths caused by scorpion stings were recorded, and the injury of 450 others due to scorpion stings. Significant agricultural and livestock losses, food, and crops were rendered useless by the floods in more than 11 villages across the affected areas (International Federation of Red Cross and Red Crescent Societies, 2022).

The main objectives of this work are flash floods analysis and assessment for two storms (November 2021 and August 2024), discuss the environmental impacts of flash floods and select appropriate mitigation methods and identify the urban areas affected by flash floods.

MATERIALS AND METHODS

The following data and software were used in the achievement of goals of this work:

- Historical climate data from the Egyptian Meteorological Authority (EMA) covering the years 1968 to 2023 for the Aswan meteorological station.
- Rainfall data from storms that occurred in November 2021 and August 2024, which were obtained from satellite data sources (GSMAP, 2000-2023 and NASA, 2024).
- Topographic maps at a scale of (1:50000) provided by the Egyptian General Survey Authority (EGSA, 1991-1997).

- Geologic maps at a scale of 1:500000 provided by Continental Oil Company (CONOCO, 1987).
- Google Earth Map (2024) for urban visual interpretation.
- Hydrologic Engineering Center-Hydrologic Modeling System, version 4 (HEC-HMS, 2010) for both analysis of storms and calculation of rainfall-runoff.

1. Site Description

The area under investigation is located along the Nile Valley to the east of Aswan city. It is bounded by latitudes 23° 45’ 00” N and 24° 15’ 00” N and longitudes 32° 38’ 00” E and 33° 22’ 00” E (Fig. 1). Four Wadis were selected to study the relation between rainfall and runoff: Wadi Abu Aggag (493 km^2), Wadi El Heta (16.47 km^2), Wadi Kimb (43.02 km^2) and Wadi Umm Boirat (102.77 km^2). These basins originated mainly from the mountainous highland of basement rocks to the east. They follow westwards to the Nile River.

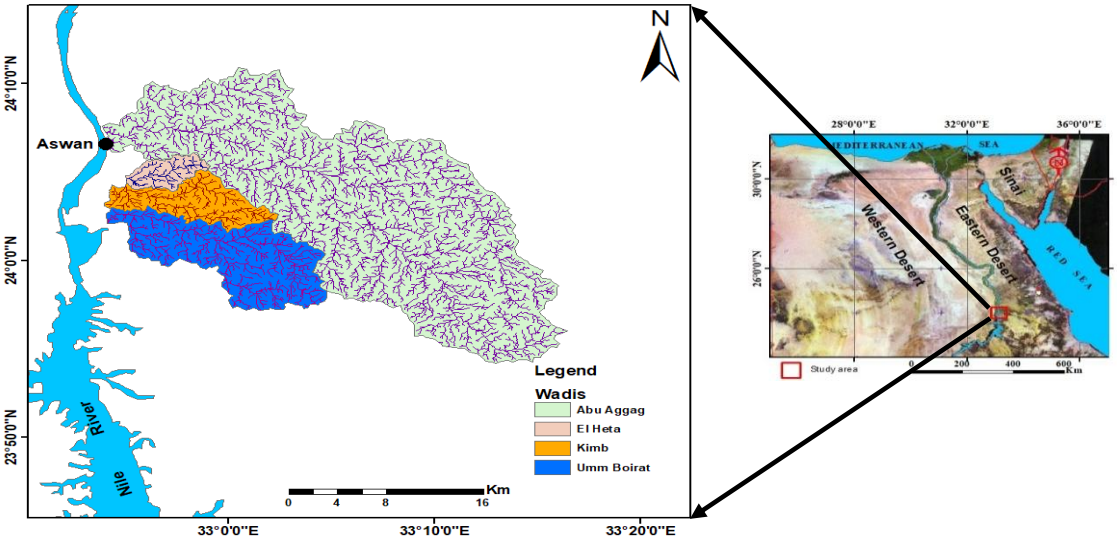

Fig. (1). Location map of the study area.

2. Meteorological Conditions

The area of study belongs to the arid zone which is characterized by very high temperatures in the summer season and a mild climate in winter season. January is the coldest month, with an average low temperature of 8.7°C. Aswan is one of the least humid cities in Egypt. The maximum relative humidity is recorded in December (39%), while the month with the least relative humidity is May (16%). The rainfall in this area is rare, but storm rainfall events can occur suddenly in the Wadis surrounding Aswan city. Table (1) shows the mean monthly climatic data collected from the Aswan meteorological station from the (EMA) during the period (1968-2023).

Table (1). Mean monthly climatic data during the period (1968-2023) (EMA).

Month	Rainfall (mm)	Evaporation (mm day^{-1})	Max. temperature (°C)	Min. temperature (°C)	Relative humidity (%)
January	2.11	9.65	22.4	8.7	36
February	2.16	12.54	24.5	10.0	29
March	2.43	16.53	29.7	14.0	22
April	3.80	19.77	35.2	19.3	19
May	1.00	22.17	38.7	23.0	16
June	0.25	23.81	41.2	25.3	17
July	0.00	22.59	40.9	26.1	20
August	0.00	21.54	40.5	25.9	22
September	0.01	20.72	39.0	23.6	24
October	0.24	18.12	35.6	20.7	27
November	0.87	12.64	28.8	15.2	34
December	0.52	10.10	24.1	10.7	39

3. Geomorphological Setting

A geomorphologic map for the area under investigation was constructed using the Digital Elevation Model (DEM) data of 30 m resolution (Fig. 2) and both the topographic and geologic maps. From this map, three geomorphologic units are discussed in the following (Fig. 3):

3.1. Flood plain

Flood plain is formed of flat lowland with an area of 135.44 km^2 and an average elevation of about 60 m above mean sea level. It is very narrow; its width in Aswan is about 300 m (El Hussein, 2021). It stretches to the west of the investigated area. Deltas of Wadi Abu Aggag, Wadi Umm Boirat represent a part of this unit. It is covered by Nile sedimentary deposits of Quaternary age.

3.2. Piedmont plain

It is Considered as an intermediate area lying between the highlands (plateau units) in the east and the Nile flood plain area in the west. Its area is about 634.6 km^2 and elevations range from 60 m to 200 m above mean sea level. It is covered by alluvium deposits derived from the mountain area to the flood plains. These deposits consist of sand, gravel and conglomerates. It belongs to the Upper Cretaceous age.

3.3. Plateau

It is a part of the Ababda plateau having an area of 2002.10 km^2 and 200-500 m elevation above mean sea level. It is considered a mountainous area that shows many mountains with different elevations such as: Jabal Bayda (322 m), Jabal Dihaysah (412 m), Jabal al Hudi (362 m) and Jabal Dihmit (508 m). It is characterized by a high and steep area. It is formed as a water shed for the studied Wadis. It belongs to the Precambrian Era.

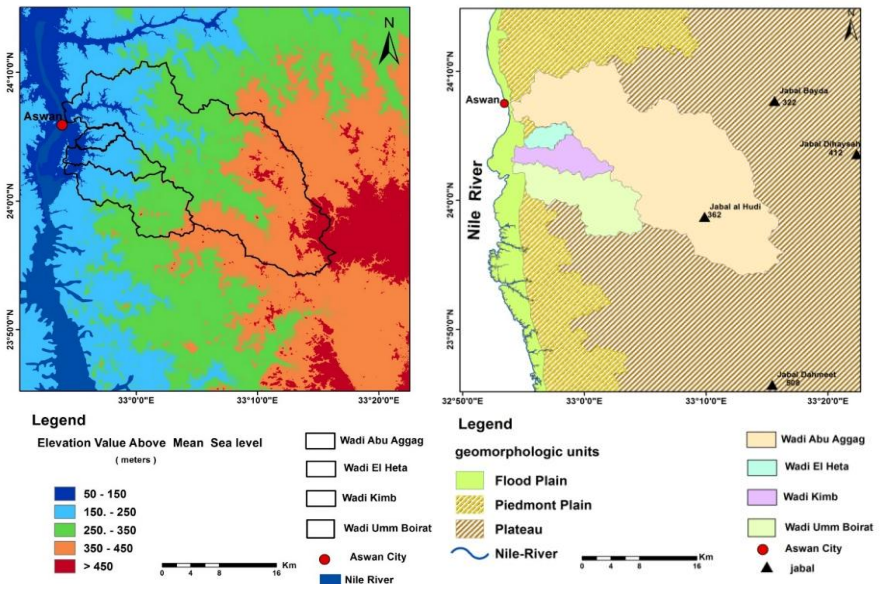

Fig. (2). Digital Elevation Model (DEM). **Fig. (3).** The geomorphologic map.

4. Geological Setting

Several authors studied the geological setting of the study area (Fourtau, 1915; El-Shazly et al., 1977; Hamdan, 1980; El Gammal et al., 2013 and Sharaka et al., 2021).

Stratigraphically, the Precambrian rocks are the main rocks in the study area representing the oldest exposed rocks in the area under investigation and overlaid by a thick sedimentary succession from Upper Cretaceous to Quaternary ages. Depending on geologic maps: Gebel Hamata, Luxor, Lake Nasser, Bernice (Scale 1:500000) (CONOCO, 1987). The exposed geologic rocks are defined as follows (Fig. 4):

4.1. Precambrian rocks

They are composed of igneous and metamorphic rocks. Diorites, grano diorites and red granites (Aswan granite) are the main components of the igneous rocks and schist with subordinate gneisses represent the metamorphic rocks.

4.2. Upper cretaceous

Consists of the Nubia group (Sharaka et al., 2021), representing Abu Aggag, Timsah and Um Barmil formations.

- Abu Aggag Formation**:** is overlying the basement rocks and underlying Timsah Formation to the northeast of Aswan at Wadi Abu Aggag. It consists of koalinitic beds, basal conglomerate, sandstones, clays, clayey sandstone and sandy clay. Its thickness is about 50 meters.

- Timsah Formation: It is uncomfortably overlying Abu Aggag Formation and underlies Umm Barmil Formation. It is fluviatile near shore marine and locally eolian sandstone. The upper part of Wadi Abu Aggag consists of sandstone and at the base consists of pale to dark grey, brownish to yellowish grey massive of laminated and moderately hard clays.
- Umm Barmil (Nubia) Formation**:** It is uncomfortably overlying Timsah Formation and consists of sandstone of continental origin and is partially covered by Quaternary sediments. It is about 60 meters thick.

4.3. Quaternary deposits

Quaternary deposits consist of accumulations of surficial materials of Wadi deposits (silt, sands gravels and rock fragments) and sand sheets covering lowlands **(**El Gammal et al., 2013). Structurally, according to geological maps and (El Hinnawi, 1965), the N-S, NNW-SSE, NW-SE and E-W faults are the main structural elements affecting the investigated area (Fig. 4).

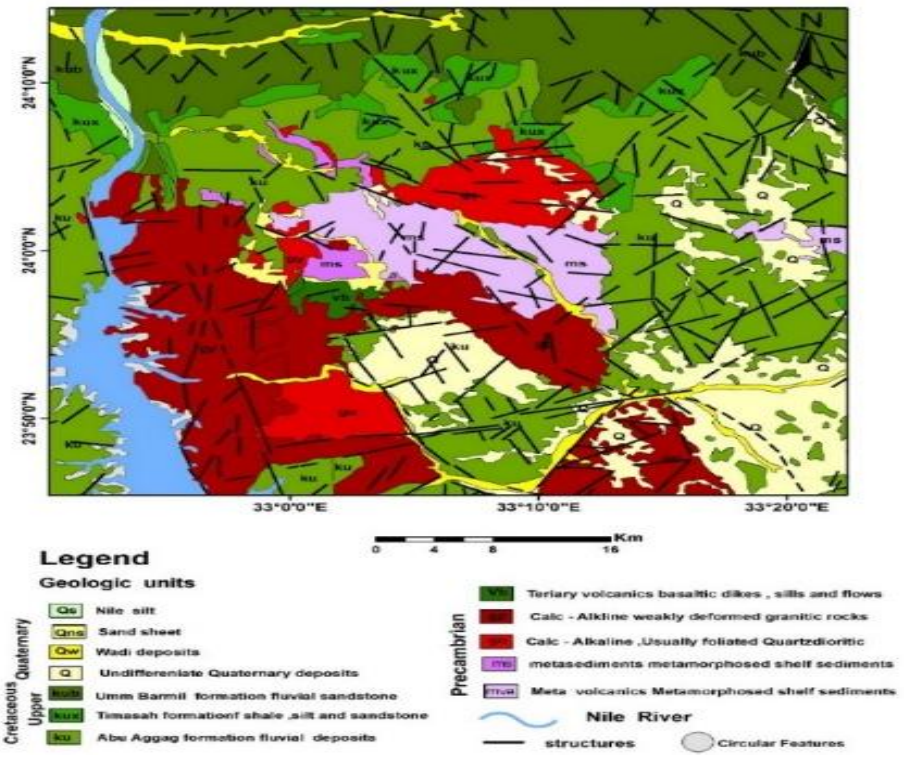

Fig. (4). Geologic map of the study area (Modified after CONOCO, 1987).

5. Morphometric Analysis of the Basins

The hydrological characteristics of the studied basins are mainly defined through their morphometric parameters. The geomorphological features are the main bases of the morphometric analysis of these basins. The

morphometric parameters of the selected Wadis were determined using the data of (DEM) that has a resolution of 30 meters. Hydrology tools of the copyright version 10.4 of the Arc/GIS Software were applied in recognizing and filling all sinks in the collected mosaic of the investigated Wadis.

The stream orders classification was done automatically through the hydrology tool (stream order option) using Strahler method (Strahler, 1957). The different parameters were measured and calculated according to (Horton, 1932 and Horton, 1945). These parameters include: i) Texture Ratio, ii) Basin, Valley Length (L_b, L_v) and Sinuosity Ratio, iii) Form Factor Ratio, iv) Compactness Ratio, v) Shape Index, vi) Circularity Ratio, vii) Elongation Ratio, viii) Bifurcation Ratio and Weighted Mean Bifurcation Ratio, ix) Drainage Density, x) Stream Frequency, xi) Relief and Relief Ratio, xii) Ruggedness Number and xiii) Length of overland flow.

6. Detection of Urban Areas

Visual interpretation of Google Maps is applied to define the urban areas in the area under investigation. The general advantage of conventional visual interpretation is its high accuracy of the results. The process of visual interpretation can be divided into the following steps:

- Visual registration of features.
- Recognition and identification of the observed features.
- Analysis, which groups the features in space using mapping.
- Finishing the interpretation with a classification

7. Rainfall Characteristics

The main elements describing the rainfall characteristics are as follows:

1. Rainfall Depth, which is the thickness of the water layer on the ground surface.
2. Duration of rainfall; it is the elapsed time from the start to the end of the event of the rainfall.
3. Rainfall intensity, expressed as water depth per unit time.
4. Frequency of rainfall which refers to the average time elapsed between occurrences of two rainfall events.

The study area was subjected to severe storms during the last century. Data of rainfall is collected from the meteorological stations and from satellite websites (GSMAP, 2000-2023 and NASA, 2024) as shown in Tables (2) and (3). It was noticed that flash floods have become more frequent, especially after 2010.

Table (2). Data of rainfall storms (2000-2024) (GSMAP, 2000-2023 and NASA, 2024).

Year	Date	Rainfall depth (mm)	Duration (h)	Intensity (mm h^{-1})	Max. rainfall h^{-1}
2000	26 Dec.	0.30	2	0.15	0.05
2001	3-4 Apr.	1.20	18	0.07	0.70
2002	27-28 Apr. Oct.	4.04	26	0.16	0.61
2003	1-2 May.	8.92	24	0.37	1.47
2004	12-13 Jan.	1.70	4	0.43	0.05
2005	22-23 Jan.	13.44	15	0.90	4.00
2006	13- May	4.30	5	0.86	1.50
2007	30 Apr.	2.70	8	0.34	1.60
2008	20-21 Jan.	13.26	18	0.74	2.22
2009	4-10 May	60.48	128	0.47	3.70
2010	17-18 Jan.	7.20	9	0.80	2.40
2011	29- Apr	1.60	3	0.53	1.20
2012	21- Oct	3.50	12	0.29	1.80
2013	26- Jan	1.00	10	0.10	0.25
2014	7-9 Mar.	27.7	54	0.51	1.67
2015	11 Sep.	7.90	7	1.13	3.03
2016	15 Mar.	15.87	15	1.06	2.42
2017	13-14 Apr.	24.01	26	0.92	2.71
2018	15-16 Jan.	47.98	28	1.71	3.53
2019	27-28 Jan.	24.00	16	1.50	4.80
2020	11-12 Mar.	11.02	30	0.37	1.10
2021	12 Nov.	18.78	5	3.76	8.43
2022	9 Jan.	10.38	18	0.58	2.06
2023	12 Jan.	4.80	7	0.69	4.60
2024	3-5 Aug.	69.72	46	1.50	14.63

Table (3). Maximum storm rainfall depth (1921 -2024).

Year	Date	Rainfall Depth (mm)
1921	10 Dec	7.80
1962	17 Aug.	4.10
1968	16 Apr.	7.20
1977	16-17 Oct.	8.60
1979	16 May	9.10
1994	11-12 Oct	7.00
1997	17 Nov.	8.60
2003	1-2 May.	8.92
2005	22-23 Apr.	13.44
2008	20-21 Jan.	13.26
2009	4-10 May	60.48
2010	17-18 Jan.	7.20
2014	7-9 Mar.	27.70
2016	15 Mar.	15.87
2017	13-14 Apr.	24.01
2018	15-16 Jan.	47.98
2019	27-28 Jan.	24.00
2020	11-12 Mar.	11.02
2021	12 Nov.	18.78
2022	9 Jan.	10.38
2023	22-23 May	9.33
2024	3-5 Aug.	69.72

8. Rainfall-Runoff Modeling

Flash floods often occur in arid regions because of excessive rainfall which occasionally causes major loss of property and life. In general, surface runoff occurs when rainfall intensity exceeds the abstractive capability of the catchment rocks, where catchment characteristics and the climatic factors influence the rainfall runoff relationship. This relationship is of particular importance for management and protection of catchment from flooding. In the present study, two heavy storms were selected to investigate the rainfall-runoff relationship. The first storm occurred on 12 November 2021, caused huge damage to the infrastructures in Aswan governorate. This storm was characterized by a short duration (5 hours), 18.78 mm rainfall depth and high rainfall intensity of 3.76 mm h^{-1}. The second storm occurred on 3-5 August 2024. This sudden storm had 69.72 mm rainfall depth and 1.5 mm h^{-1}. rainfall

intensity. Table (4) shows the collected storm data for the rainfall storm in November 2021 and August 2024. The Hydrologic Engineering Center-Hydrologic Modeling System, version 4 (HEC-HMS, 2010) was used to analyze and simulate surface runoff during storms. Specifically, it was applied to the storms that occurred in November 2021 and August 2024 across four Wadis. To establish the rainfall-runoff relationship, methods for estimating losses and calculating lag time were used to determine the appropriate parameters. The software includes three main components:

- Basin Model: Covers key elements of the water system, such as sub-basin area, lag time, and initial losses.
- Meteorological Model: Focuses on rainfall data, including its amount, distribution, and duration.
- Control Specifications: Defines the period, time step, and duration of the storm being analyzed.

Table (4). Storm data for studied wadis.

Period	Rainfall depth (mm)	Storm duration (h)	Intensity (mm h^{-1})	Maximum rainfall in hour (mm)
12 Nov. 2021	18.78	5	3.76	8.42
3-5 Aug. 2024	69.72	46	1.5	14.63

RESULTS AND DISCUSSION

1. Morphometric Characteristics of Drainage Basins

The morphometric analysis of drainage basins of the four Wadis; Abu Aggag, El-Heta, Wadi Kimb and Wadi Umm Boirat are measured and calculated (Tables 5 and 6 and Fig. 5). These parameters revealed the following

1.1. Texture ratio

The texture ratio (Tr) is classified into four categories (Morisawa, 1957):

1) Less than 8 streams km^{-1} (coarse texture),
2) From 8 to 20 streams km^{-1} (medium texture),
3) From 20 to 200 streams km^{-1} (soft texture) and
4) More than 200 streams km^{-1} (very soft texture).

The texture ratio of Wadi Abu Aggag is about 15.85 streams km^{-1} (medium texture, category 2), while Wadis El-Heta, Kimb and Umm Boirat have coarse texture (category one) indicating that they have a good chance for groundwater recharge.

1.2. Basin and valley lengths (L_b and L_v) and sinuosity ratio (Si)

The basin and valley lengths (L_b and L_v) and sinuosity ratio (Si) were calculated according to Mueller (1968)**.** The sinuosity ratio (Si) is 1.36 at Wadi Abu Aggag, 1.25 at Wadi El-Heta, 1.2 at Wadi Kimb and 1.27 at Umm Boirat.

The (Si) of these Wadis indicates less meandering of main channels of the drainage basins resulting in an increase in the effectiveness of flooding.

1.3. Form factor ratio (FFR)

The (FFR) of the four Wadis are 0.264 at Abu Aggag, 0.415 at El-Heta, 0.216 at Kimb and 0.258 at Umm Boirat. These low values result in an elongation in the shape of these basins and have lower peak runoff of longer duration over their areas.

Table (5). Basic data of the selected wadis.

Parameter		Name of the wadis			
		Wadi Abu Aggag	**Wadi El Heta**	**Wadi Kimb**	**Wadi Umm Boirat**
Area (A) (km^2)		493.0	16.47	43.02	102.77
Perimeter (P) (km)		137.780	19.72	41.11	62.02
Basin width (w) (km)		9.90	2.62	3.10	4.90
Order of trunk channel		6^{th}	4^{th}	5^{th}	5^{th}
Direction of main trunk		SE-NW	E-W	E-W	SE-NW
First order	Stream no.	1702	58	144	342
	Length (km)	633.32	17.62	54.79	134.45
Second order	Stream no.	374	15	30	74
	Length (km)	319.83	12.46	21.75	60.51
Third order	Stream no.	86	2	7	19
	Length (km)	141.2	5.40	14.41	28.93
Fourth order	Stream no.	17	1	2	3
	Length (km)	79.40	2.25	12.19	21.78
Fifth order	Stream no.	4		1	1
	Length (km)	52.43	-	3.53	11.34
Sixth order	Stream no.	1			
	Length (km)	23.17	-	-	-

Table (6). Morphometric parameters of the studied Wadis

Parameters	Unit	Name of the wadis			
		Wadi Abu Aggag	**Wadi El-Heta**	**Wadi Kimb**	**Wadi Umm Boirat**
Sum of stream numbers ($\sum N_u$)		2184	76	184	439
Sum of stream lengths ($\sum L_u$)	km	1249.4	37.71	106.67	257.01
Valley length (L_V)	km	58.59	7.91	16.9	25.4
Basin length (L_b)	km	43.2	6.3	14.1	19.95
Texture ratio (Tr= Nu/P)	km^{-1}	15.85	3.85	4.48	7.07
Sinuosity ratio ($S_i= L_v/L_b$)		1.36	1.25	1.20	1.27
Form factor ratio (FFR= ($A/ L_b^{2)}$		0.264	0.415	0.216	0.258
Compactness ratio (SH=P/2($\sqrt{\pi}$A)		1.751	1.371	1.769	1.727
Shape index (Ish= $1.27A/L_b^2$)		0.335	0.527	0.275	0.328
Circularity ratio (Rc= $4\pi A/P^2$)		0.326	0.532	0.319	0.336
Elongation ratio (Re= ($2\sqrt{A/\pi}$)/ L_b		0.5801	0.727	0.525	0.573
Bifurcation ratio Rb= ($\sum N_u / \sum N_{u+1}$)		4.442	4.456	3.646	4.462
Weighted mean bifurcation ratio WMRb= $\sum(Rb_u/Rb_{u+1})$ $(Nu + N_{u+1})/(\sum N)$		4.532	4.432	4.604	4.545
Drainage density (D= ($\sum L_u/A$)	km^{-1}	2.534	2.290	2.480	2.50
Stream frequency (F= ($\sum N_u /A$)	km^{-2}	4.430	4.614	4.278	4.272
Upstream elevation	m	390	211	257	342
Downstream elevation	m	95	104	110	111
Relief (R)	m	295	107	147	231
Relief ratio ($R_f= R/L_b$)	$m\ m^{-1}$	0.007	0.017	0.010	0.012
Ruggedness no. (Rn=R*D)		0.748	0.245	0.365	0.578
Length of overland Flow (Lo = 1/2D)	km	0.197	0.218	0.202	0.200

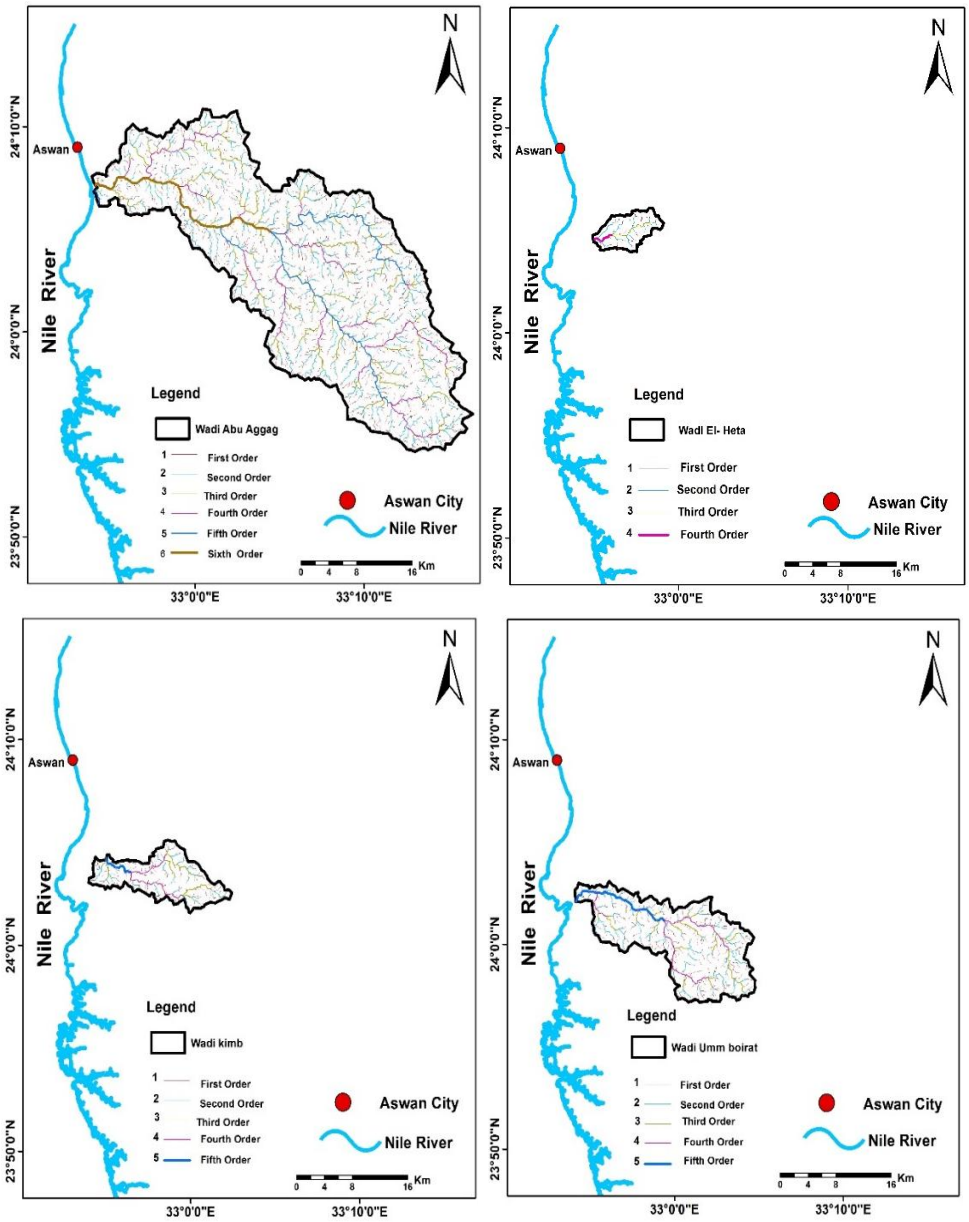

Fig. (5). Stream orders map of studied wadis.

1.4. Compactness ratio (CR)

The drainage basins have calculated compactness ratios (CR) of 1.751 at Wadi Abu Aggag, 1.371 at Wadi El-Heta, 1.769 at Wadi El Kimb and 1.727 at Wadi Umm Boirat. These values indicate that these basins are elongated in shape.

1.5. Shape index (Ish)

It ranges from 0.335 at Wadi Abu Aggag to 0.525 at Wadi El-Heta. These values indicate that the basins lengths are short, which increases the probability of flooding.

1.6. Circularity ratio (Rc)

Wadis Abu Aggag, El-Heta, Kimb and Umm Boirat have (Rc) values of 0.326, 0.532, 0.319 and 0.336, respectively. This reflects the dominance of elongation character for all studied basins. This means a low discharge of runoff which is considered as a favorable condition for groundwater recharge.

1.7. Elongation ratio (Re)

The calculated (Re) values are 0.580, 0.727, 0.525 and 0.573 for Wadis Abu Aggag, El-Heta, Kimb and Umm Boirat, respectively. These results of the four basins indicate that they are near elongation and far from circulation.

1.8. Bifurcation ratio (R_b) and **weighted mean bifurcation ratio (WMR_b)**

The bifurcation ratio (R_b) ranges between 3.646 at Wadi kimb to 4.462 at Wadi Umm Boirat. On the other hand, the values of the weighted mean bifurcation ratio (WMR_b) are 4.532 for Wadi Abu Aggag, 4.432 for Wadi El-Heta, 4.604 for Wadi Kimb and 4.545 for Wadi Umm Boirat. These high values indicate that all basins have a good chance for groundwater to recharge.

1.9. Drainage density (D)

The values of (D) range between 2.534 km^{-1} at Wadi Abu Aggag and 2.290 km^{-1} at Wadi El-Heta. These low values reflect the infiltration of the rainfall into the groundwater which increases the groundwater storage.

1.10. Stream frequency (F)

The values of stream frequency (F) range from 4.272 at Wadi Umm Boirat to 4.614 at Wadi El-Heta.

1.11. Relief and Relief Ratio (R and R_f)

Relief (R) values in the studied basins range between 107 m (Wadi El-Heta) and 295 m (Wadi Abu Aggag). Relief ratio (**R_f**) values range between 0.007 (Wadi Abu Aggag) and 0.017 (Wadi El-Heta).

1.12. Ruggedness Number (Rn)

The ruggedness number (Rn) varies between 0.245 at Wadi El-Heta and 0.748 at Wadi Abu Aggag). These low values indicate a gentle slope of all basins and moderate relief. This means less runoff and good potential for groundwater recharging.

1.13. Length of overland flow (Lo)

The calculated values of (Lo) range between 0.218 km (Wadi El-Heta) and 0.197 km (Wadi Abu Aggag). These values indicate that the studied basins haven't any significant difference between them.

According to the results of all calculated morphometric parameters, we can conclude that the studied basins have almost the same characteristics. These basins are great examples of areas that have elongated shapes with a

long time of concentration, which means they can effectively recharge groundwater and consequently increase its potential.

2. Urban Areas

The estimated residential development areas from Google maps (2024) in the outlets of the studied Wadis reach 38.32 km^2 (Fig. 6). This expansion in urban areas led to an increase in the impervious areas, changed the hydrologic cycle and consequently reduced the infiltration rate of this area. It can be noticed from Fig. (6), that the urban areas cover the outlets of the studied basins. The studied Wadis don't debouche in the Nile due to the huge amount of buildings in the last decade. Accordingly, flash floods cause great damages to the infrastructure of the urban areas.

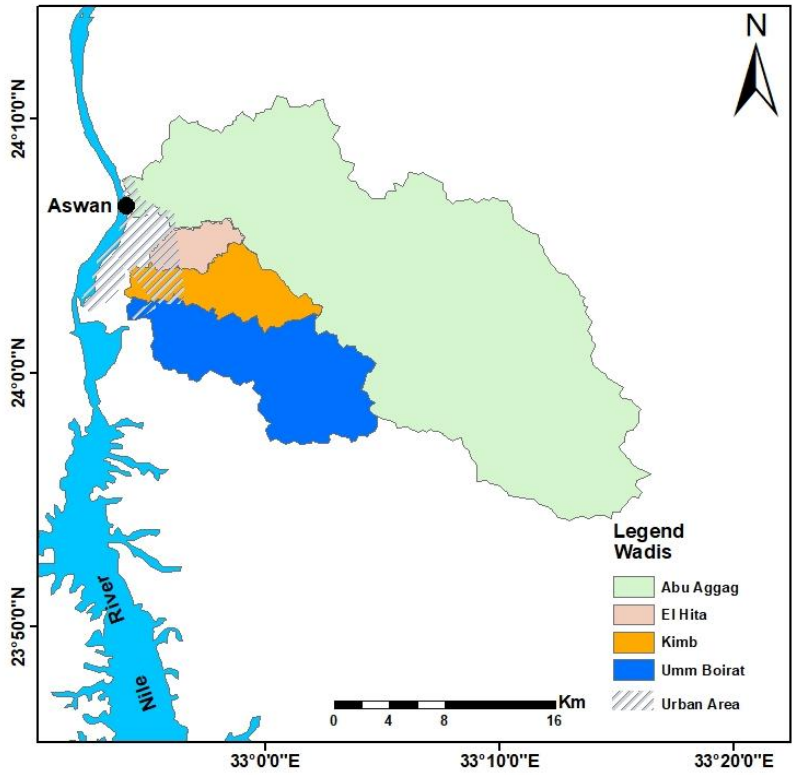

Fig. (6). A map showing the urban areas (2024).

3. Rainfall Characteristics Discussion

From the rainfall data (Tables 2 and 3 and Fig. 7), the following points can be concluded:

- The period from 2000 to 2024 represents a rainy period where the rainfall falls almost every year.

- The rainfall intensity ranges between 0.07 mm h^{-1} (2001) to 3.76 mm h^{-1} (2021).
- The maximum hourly rainfall varies from 0.05 mm (2000) to 14.63 mm (2024).
- The analysis of rainfall occurrence depends fundamentally on the rainfall depth and duration.
- Although the rainfall storm of 2009 represents a maximum rainfall depth (60.48 mm), but this amount falls in a long duration of 128 hours (more than 5 days) as shown in its hyetograph (Fig. 8). Due to this long duration, the calculated rainfall intensity has a small value (0.47 mm h^{-1}). Compared with the storm of 2021, which fell in only 5 hours, the calculated rainfall intensity was 3.76 mm h^{-1} (Fig. 9).
- An unexpected rainfall occurred in August 2024, which represents one of the driest months of the year. This storm lasted for three continuous days (3-5 August) with a total rainfall of 69.72 mm. This storm is considered one of the phenomena of climate change in Egypt. Fig. (10) shows the hyetograph of this storm.

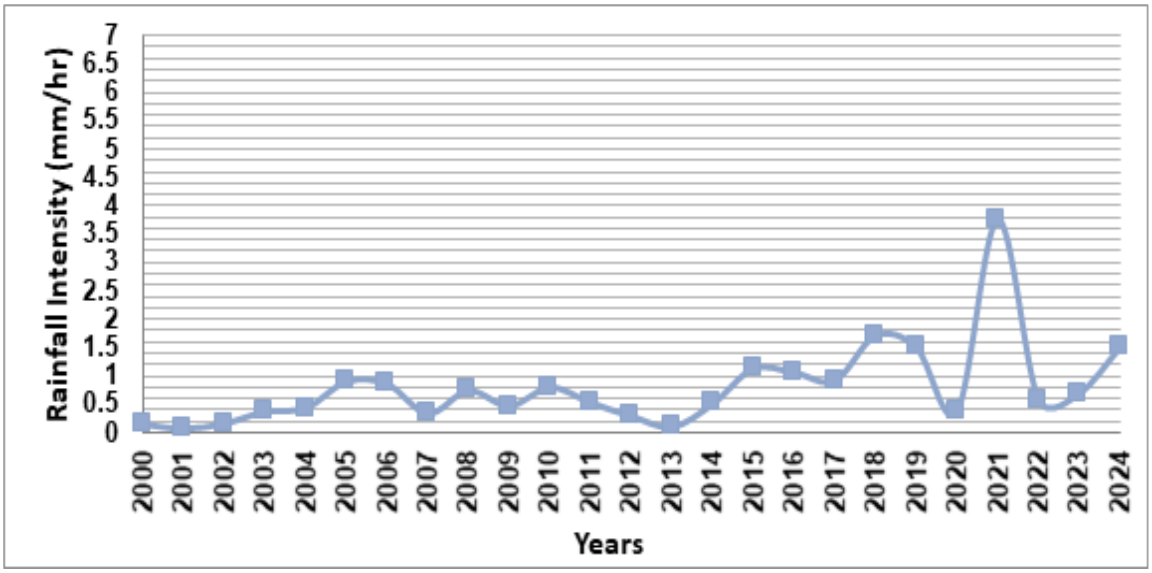

Fig. (7). Rainfall intensity for different storms (2000- 2024).

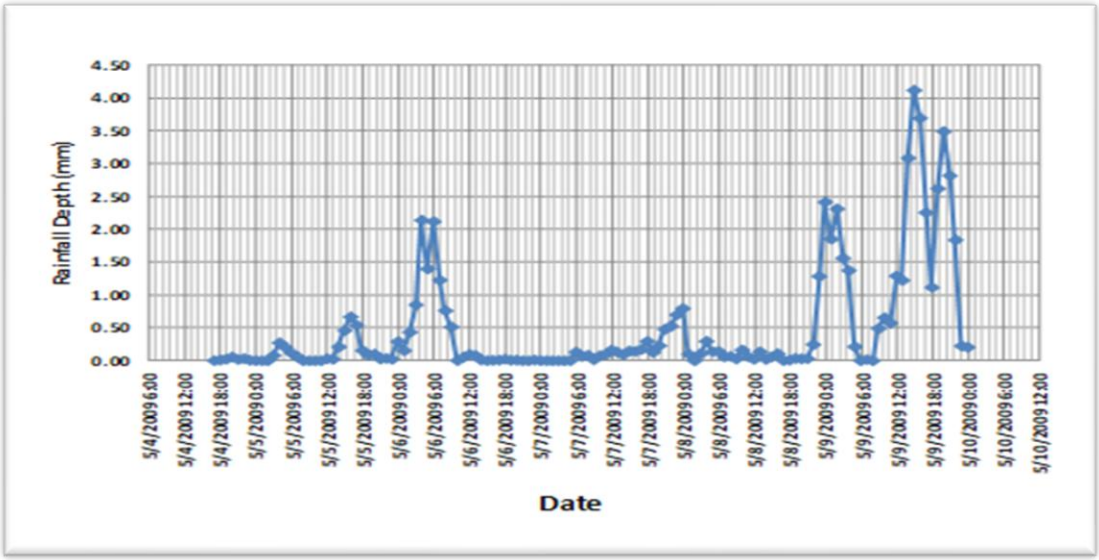

Fig. (8). Hyetograph for rainfall storm May 2009.

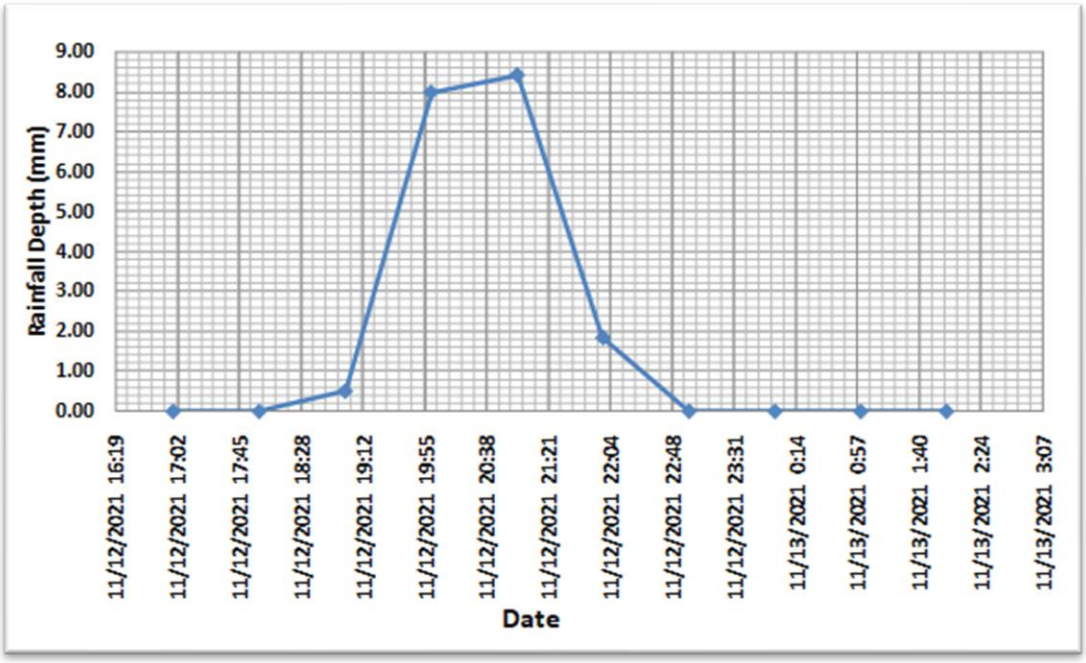

Fig. (9). Hyetograph for rainfall storm, November 2021

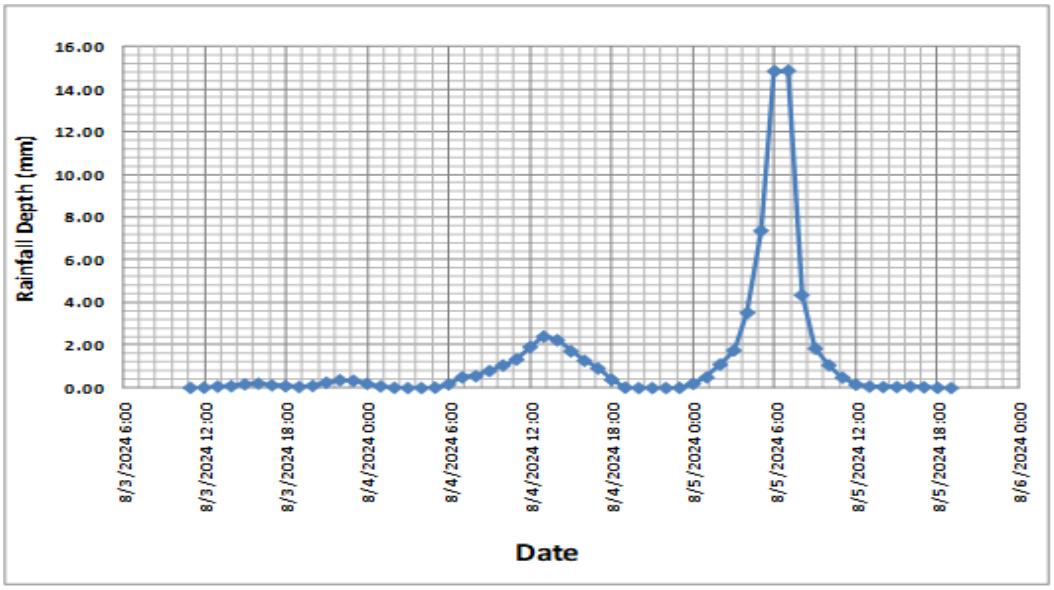

Fig. (10). Hyetograph for rainfall storm August 2024.

4. Watershed Modeling

HEC-HMS was used to generate the runoff hydrograph of the studied basins. The input data include catchment data, rainfall data and losses data. Muskingum method (Al-Humoud and Esen, 2006) was adopted as the routing method.

4.1. Model input data

a) Catchment area

Based on morphometric and geologic characteristics of the four Wadis, each Wadi was treated as one basin. Table (7) illustrates the following morphometric parameters of the four basins: the catchment area (km^2), basin length (km), valley length (km), minimum and maximum elevation (m) and average slope ($m\ m^{-1}$). The results reveal that Wadi Umm Boirat is the largest in area with a total area of about 103 km^2, where Wadi El Hita is the smallest with area of about 16 km^2. This data is considered as input data for the model.

Table (7). Main data of studied basins.

Name of Basin	Area (km^2)	L_b (basin length) (km)	L_v (valley length) (km)	Max. Elevation (m)	Min. Elevation (m)	Slope ($m\ m^{-1}$)
Wadi Abu Aggag	493	58.59	43.2	390	95	0.007
Wadi El Heta	16.47	7.91	6.3	211	104	0.17
Wadi Kimb	43.02	16.9	14.1	257	110	0.012
Wadi Umm Boirat	102.77	25.4	19.95	342	111	0.010

b) Rainfall data

The recorded data of storms (12 November 2021, 3-5 August 2024) for the studied basins were used in the HEC-HMS model in form of incremental precipitation (depth of precipitation for each time interval). The start and end dates and times of the storm are entered as input data in the model. The precipitation–time distribution is entered with a time step of one hour.

c) Losses calculations

The rainfall loss is rainfall which doesn't contribute to direct runoff (Ponce, 1989). The Soil Conservation Service method (SCS, 1986) was used to calculate the basins losses. It requires the curve number (CN) values, initial abstraction and percent of impervious area. This approach is popular because of its application to ungagged areas. The CN is based on the area's hydrologic soil group and land use. The CN varies from 0 to 100, higher values indicate higher surface runoff and lower values indicate higher soil infiltration with lower surface runoff. According to the percentage of the total sub-catchment area with its corresponding CN a weighted average CN is calculated according to the following equation (Table 8):

$$\boldsymbol{CN} = \frac{\sum_{i=1}^{k} \boldsymbol{A_i CN_i}}{\sum_{i=1}^{k} \boldsymbol{A_i}} \ldots\ldots\ldots\ldots (\mathbf{1})$$

Where:

CN_i corresponds to the appropriate CN for the part of the watershed that has an area

A_i is the percentage of the sub-basin, which is directly connected impervious area, can be calculated according to the geological map of the study area (Table 8). No loss calculations are carried out on the impervious area; all precipitation on that portion of the sub-basin becomes excess precipitation and is subject to direct runoff (NRCS, 2007).

The initial abstraction (Ia) defines as the amount of precipitation that must fall before surfacing excess results. It is empirically derived from the maximum soil water retention (S), which is related to the soil drainage characteristics (e.g. CN values).

(S) accounts for the total amount of water retained in the drainage basin during the rainfall event**.** The equations used for these calculations are as follows:

$$S = \frac{25400}{CN} - 254 \ldots\ldots\ldots\ldots\ldots (2)$$

$$Ia = 0.2 \times S \ldots\ldots\ldots\ldots\ldots\ldots (3)$$

Where:

S = the potential retention parameter or surface storage after runoff begins (mm),

Ia = Initial abstraction (mm)

Table (8). CN values for the studied wadis.

Name of basin	Geological classification	Basin area (km^2)	Sub-basin area (km^2)	Sub-basin area (%)	CN	Weighted CN
Wadi Abu Aggag	Basement	493	233.15	47.29	92	83.00
	Upper Cretaceous		222.69	45.17	77	
	Quaternary		38.03	7.71	63	
Wadi El Heta	Basement	16.47	4.35	26.41	92	81.00
	Upper Cretaceous		12.12	73.5	77	
	Quaternary			0.00	63	
Wadi Kimb	Basement	43.02	13.36	76.24	92	81.15
	Upper Cretaceous		28.80	12.39	77	
	Quaternary		1.41	11.37	63	
Wadi Umm El-Boirat	Basement	102.77	78.35	31.06	92	86.84
	Upper Cretaceous		12.73	66.95	77	
	Quaternary		11.69	3.28	63	

d) Time of concentration and lag time calculation

According to Granato (2010), lag time (T_L) can be defined as the time interval from the center of mass of rainfall excess to the center of the peak of runoff hydrograph. Mockus (1957) estimated the lag-time by a value of 0.6 T_c, where T_c is the time of concentration and it is calculated by applying Kirpich equation (Subramanya, 1984) as follows:

$$T_c = 0.0194 \frac{L^{0.77}}{S^{0.385}} \quad \text{..... (4)}$$

Where:

T_c= Time of concentration (min.)

L = Basin length, which is measured along the mainstream from the outlet to the divide (m)

S = Slope of the basin (m m^{-1})

e) Routing Method

Routing is the movement of the runoff from the different watersheds outlets throughout the system along the stream, and ultimately to the outlet or sink of the entire watershed system. The routing method used in this work is the Muskingum method (Al-Humoud and Esen, 2006), which uses a simple conservation of mass approach to route through the stream reach (NRCS, 2007). By adding a travel time for the reach (K) and a weighting coefficient (X), it is possible to approximate attenuation.

The value of X depends on the shape of the wedge storage to be modeled and ranges from 0 to 0.3 with a mean value near 0.25 (Chow et al., 1988). K is the time required for an incremental flood wave to traverse its reach and it may be estimated as the observed time of travel of peak flow

through the reach (Veissman and Lewis, 2003). The following values were used in the model:
X= 0.25 K = 0.50 hours and the input data used in the hydrologic model is illustrated in Table (9).

Table (9). The input parameters used in HEC-HMS model.

Name of basin	Concentration time (T_c) (min)	Lag time (T_L) (min)	CN	Potential abstraction (S) (mm)	Initial loss Ia (mm)
Wadi Abu Aggag	486.14	291.68	83.00	52.01	10.40
Wad El Heta	78.45	47.07	81.00	62.31	12.46
Wadi Kimb	233.75	140.25	81.14	59.04	11.81
Wadi Umm Boirat	166.81	100.08	86.84	38.49	7.70

5. Generation of Hydrograph

The main goals of this work are the identification of the rainfall-runoff relationship and the estimation of the runoff depth, runoff volume, and runoff coefficient (Table 10).

The depth of runoff water above the ground surface is defined as the runoff depth. The runoff coefficient is the ratio of the total depth of runoff to the total depth of rainfall and represents the amount of rainfall transmitted to runoff (Wanielista and Yousef, 1993). This coefficient varies with topography, land use, vegetal cover, soil type and moisture content of the soil (Texas Department of Transportation, TxDOT, 2002) and is calculated using the following equations (Ponce, 1989):

$$\text{Runoff Depth} = \frac{\text{Runoff Volume}}{\text{Drainage Area}} \dots\dots\dots\dots (5)$$

$$\text{Runoff Coefficient} = \frac{\text{Runoff Depth}}{\text{Rainfall Depth}} \dots\dots\dots . (6)$$

Table (10). Results of selected wadis for hydrograph generation using EC-HMS (Storms Nov. 2021 and Aug. 2024).

Name of basin	Storm 2021				Storm 2024			
	Peak discharge (m^3/s)	Runoff volume (10^3 m^3)	Runoff depth (mm)	Runoff coeff. (%)	Peak discharg (m^3 s^{-1})	Runoff volume (10^3 m^3)	Runoff depth (mm)	Runoff coeff. (%)
Wadi Abu Aggag	119.8	3175.6	6.44	34.30	515.8	15618.6	31.68	45.44
Wadi El Heta	5.20	39.7	2.41	30.02	44.0	663.0	40.26	57.75
Wadi Kimb	7.0	103.6	2.41	30.02	78.8	1769.7	41.14	59.00
Wadi Umm Boirat	43.1	663.5	6.45	37.62	213.8	4919.2	47.87	68.66

The estimated parameters were used in the generation of the runoff hydrographs for each Wadi. Fig. (11) is a schematic presentation of the basins. The discussion of the results for the two selected storms is as follows (Table 10 and Fig. 12 and 13):

- As a result of the November 2021 storm, which has 18.78 mm as a total depth and 5 hours duration, the results show that the maximum flows in Wadi Abu Aggag was 119.8 $m^3 s^{-1}$ and total runoff volume 3175.6 $x10^3$ m^3.
- The unexpected storm of August 2024 on Aswan city and its vicinity produces a huge amount of runoff water, especially in Wadi Abu Aggag. The rainfall was 69.72 mm and duration of 46 hours produced a runoff water (15618$x10^3$ m^3), with maximum flow (515.8 m^3 s^{-1}). This storm indicates noticeable climate change in Egypt.
- Although Wadi Abu Aggag represents the biggest Wadi in the study area (493 km^2), the other studied Wadis, produce a large amount of runoff as well. Wadi El-Heta (16.47 km^2) in storm of November 2021, the runoff volume was 36.7$x10^3$ m^3, with discharge equal to 5.20 m^3 s^{-1}. In storm of August 2024, the volume of runoff was 663$x10^3$ m^3, with discharge equal to 44.0 m^3 s^{-1}. So, these Wadis must be taken into consideration in any development in this area.
- It is recommended to collect and update sufficient data about the basins to avoid flood risks that may harm inhabitants.

Avoid establishing any infrastructure below dangerous cliffs or on steep ridges to avoid any dangers that may occur.

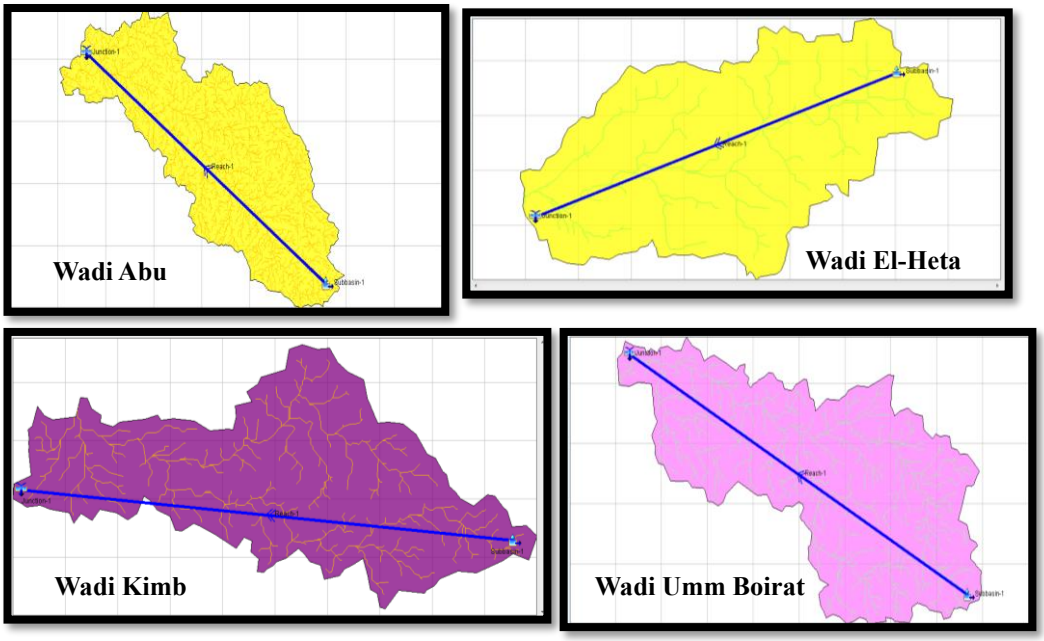

Fig. (11). Schematic presentation for the studied wadis.

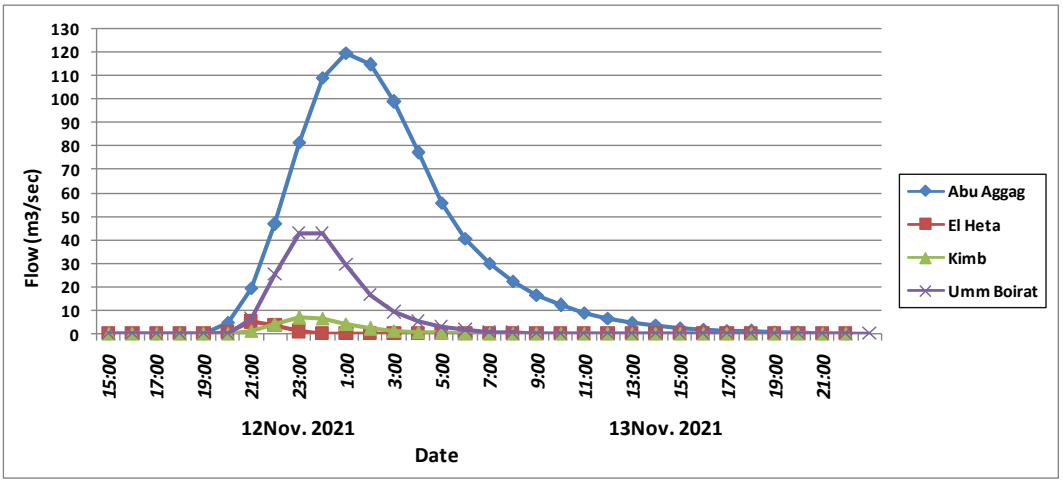

Fig. (12). Compiled hydrographs for the studied wadis (Storm Nov. 2021).

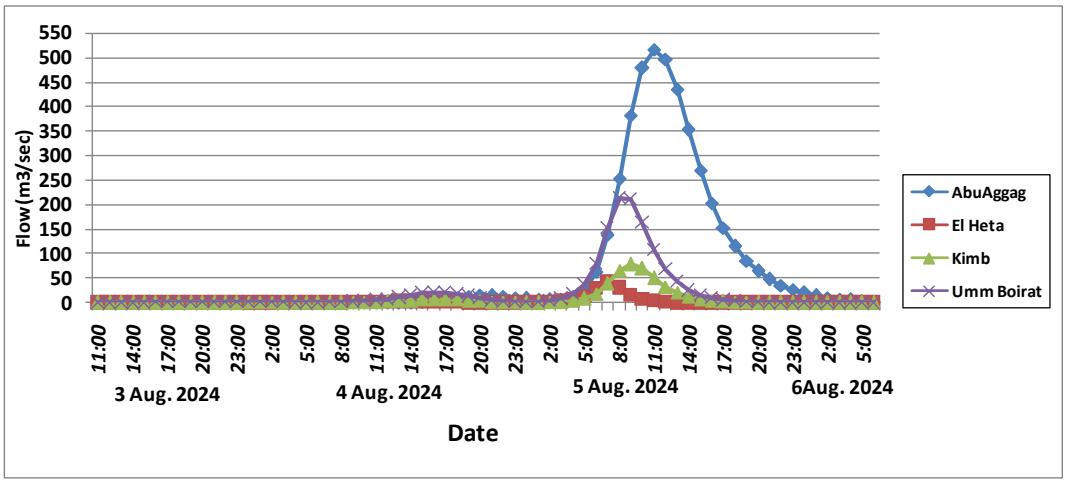

Fig. (13). Compiled hydrographs for the studied wadis (Storm Aug. 2024).

CONCLUSION AND RECOMMENDATION

From the results of the above investigation, the following can be distinguished:

1. All the studied basins have almost the same characters. These basins reflect an ideal case of elongation with high time of concentration and hence high groundwater potentialities**.**
2. The peak flow in Wadi Abu Aggag, was 119.8 m^3 s^{-1} and total runoff volume 3175.6 x 10^3 m^3 according to the November 2021 event. On the other hand, storm of August 2024 produces runoff water 15618 x 10^3 m^3, with maximum flow 515.8 m^3 s^{-1}.

3. Although Wadi Abu Aggag represents the biggest Wadi in the study area (493 km^2), but also the other studied Wadis, which are relatively small compared with Wadi Abu Aggag, also produce a large amount of runoff. Wadi El Heta (16.47 km^2) in the storm of November 2021, the runoff volume was 36.7 x 10^3 m^3, with discharge equal to 5.20 m^3 s^{-1}. In the storm of August 2024, the runoff volume was 663 x 10^3 m^3, with discharge equal to 44.0 m^3 s^{-1}. So, these Wadis must be taken into consideration in any development in this area.
4. It is recommended to collect and update sufficient data about the valley basins to avoid floods risk that may cause harm to the population.
5. Avoid establishing any infrastructure below cliffs or on steep ridges to avoid any probable risk that may occur.
6. Remove any random settlements built in the main trunk of the Wadis.
7. There is a great lack of meteorological data in this area, so installation of telemetric meteorological stations is recommended.
8. Using geotechnical studies to select the most suitable places for building houses and avoid building in areas threatened by serious torrents.
9. It is recommended to construct detention dams in the upstream area of Wadis El Heta, Kimb and Umm Boirat.
10. In the outlet of Wadi Abu Aggag, it is recommended to construct storage dams to protect the urban areas from the occasional flash flood risk and replenishment of groundwater behind these dams.

ACKNOWLEDGEMENT

The authors would like to thank the Desert Research Center (DRC) for supporting this research with all the capabilities and needs to complete this work**.**

REFERENCES

Al-Humoud, J.M. and I.I. Esen (2006) Approximate method for the estimation of Muskingum flood routing parameters, Water Resources Management, 20: 979-990.

Chow, V.T., D.R. Maidment and L.W. Mays (1988). Applied Hydrology. McGraw-Hill series in water resources and environmental engineering. ISBN 0-07-100174-3.

CONOCO and the Egyptian general petroleum company (EGPC) (1987). Geological maps of Egypt.

EGSA (1991-1997). Egyptian General Survey Authority. Topographic maps of Egypt scale, 1: 50000.

El Gammal, E.A., S.M. Salem and O.G. Reinhard (2013). Geology, Morphotectonics and Geophysical Interpretation of Wadi Garara

Graben, East Aswan Egypt, Using Landsat Images. Australian Journal of Basic and Applied Sciences, 7 (1): 263-277.

El Hinnawi, E. (1965). Contributions to the study of Egyptian (U.A.R.) Iron-ores. Economic Geology. 60 (7): 1497-1509.

El Hussein, M. (2021). Urban Geomorphology and Its Impact on Changing Land Uses in Aswan Using Information Systems Technology and Remote Sensing. Journal of the College of Arts, Qena, 30 (5): 1952-2032.

El-Shazly, E.M., F.A. Bassyouni and M.L. Abdel Khalek (1977). Geology of the Greater Abu Swayel area, Eastern Desert Egypt. Egyptian Journal of Geology, 19: 1-41.

EMA (1968-2023). Egyptian Meteorological Authority, Cairo, Egypt. Available online at: www.nwp.gov.eg/

Fourtau, R. (1915). Contribution aletude des depots Nilotiques., Mémoires présentés à l'Institut Egyptien-8.1915, LeCaire, Tome 8.

Google Earth Map (2024). DATA SIO, NOAA, U.S. Navy, NGA, GBECO Image Landsat, Copernicus.

Granato, G.E. (2010). Methods for development of planning-level estimates of storm flow at unmonitored sites in the conterminous United States. Washington, D.C., U.S. Department of Transportation, Federal Highway Administration.

GSMAP (2023). Available online at: https://sharaku.eorc.jaxa.jp/GSMaP/index.htm

Hamdan, G. (1980). Personality of Egypt. In 'Part One, World of Books', Cairo.

HEC-HMS (2010). Hydrologic Modeling System HEC-HMS. In 'version 4 US Army Corps of Engineers', Institute for Water Resources, Hydrologic Engineering Center, Davis, California.

Horton, R.E. (1932). Drainage basin characteristics. Eos, Transactions American Geophysical Union, Union, 13 (1): 350- 361.

Horton, R.E. (1945). Erosional developments of streams and their drainage basins-hydrophysical approach to quantitative morphology. Geological Society of America Bulletin, 56 (3): 275-370.

International Federation of Red Cross and Red Crescent Societies (2022). Final Report, 31 May. Available online at: www.ifrc.org.

Mockus, V. (1957). Use of storm and watershed characteristics in synthetic hydrograph analysis and application. Paper presented at the annual meeting of AUG Pacific Southwest Region, Washington, DC, USA.

Morad, N.A., S.M.M. Ibrahem and N.A. Youssef (2020). Assessment of Flash Flood "April 2018" and its Effect on Wadi Degla and Wadi El-Halazouni - East Cairo - Egypt. Egyptian Journal of Desert Research, 70 (1): 25-57.

Morisawa, M.E. (1957). Accuracy of determination of stream lengths from topographic maps. Transactions American Geophysical Union, 38 (1): 86-88.

Mueller, J.E. (1968). An introduction to the hydraulic and topographic sinuosity indexes. Annals of the Association of American Geographers, 58 (2): 371-385.

NASA (2024). Available online at: https://power.larc.nasa.gov/data-access-viewer/

NRCS (2007). Natural Resources Conservation Service. In 'National Engineering Handbook': Chapter 16 Hydrographs. Washington, DC.

Ponce, V.M. (1989). Engineering Hydrology, Principle and practices. Prentice-Hall, New Jersey, USA.

Saber, M., S. Kantoush, M. Abdel Fatah and T. Sumi (2017). Assessing Flash Floods Prone Regions at Wadi Basins in Aswan, Egypt. DPRI Annuals, 60 B: 853-863.

Sharaka, H.K., H.M. ElDesoky, M.W. AbdelMoghny, N.A. Abdel Hafez and S.A. Abu-Ellbah (2022). Geological, Mineralogical and Physical properties of Aswan Kaolinitic Clays, Egypt, Implications for Industrial Applications. Jordan Journal of Earth and Environmental Sciences, 13 (1): 64-73.

Soil Conservation Service (SCS) (1986). Hydrology guide for use in watershed planning. In 'SCS National engineering handbook, Section 4: Hydrology'. US Department of Agriculture, Soil Conservation Service, Engineering Division, Washington.

Strahler, A.N. (1957). Quantitative analysis of watershed geomorphology. Transactions of the American Geophysical Union, 38: 913-920.

Subramanya, K. (1984). Engineering Hydrology. In 'Tata Mcgraw-Hill publishing company limited', New Delhi, India, pp. 16.

Texas Department of Transportation (TxDOT) (2002). Hydraulic Design Manual. In 'TxDOT Hydraulics Branch of the Bridge Division', Austin, TX p. 78701.

Veissman, W. and G.L. Lewis (2003). Introduction to Hydrology. In '5th Ed. Prentice Hall: Upper Saddle River, NJ', pp. 612.

Wanielista, M.P. and Y.A. Yousef (1993). Stormwater Management. John Wiley and Sons, Inc., New York.

Youssef, M., B. Pradhan, A.F.D. Gaber and M.F. Buchroithner (2009). Geomorphological hazard analysis along the Egyptian Red Sea coast between Safaga and Quseir. Natural Hazards and Earth System Sciences, 9: 751-766.

دراسات هيدرولوجية لبعض الوديان المختارة بمحافظة أسوان – مصر

سوسن مصيلحي محمد إبراهيم[1]*، نهلة عبد المنعم مراد[1] ونعمات عبد المنعم عبد الغفار[2]
[1]قسم الهيدرولوجيا، مركز بحوث الصحراء، المطرية، القاهرة، مصر
[2]قسم الجيولوجيا، مركز بحوث الصحراء، المطرية، القاهرة، مصر

تتناولت هذه الدراسة اختيار عاصفتين تسببتا في أضرار جسيمة بمدينة أسوان (نوفمبر ٢٠٢١ وأغسطس ٢٠٢٤) لدراسة العلاقة بين الهطول المطري والسيول بأودية مدينة أسوان. وقد تم اختيار أربعة أودية هي: أبو عجاج، والحيتا، وكيمب، وأم بويرات لهذا الغرض. وكشف التحليل المورفومتري أن هذه الأودية ذات أشكال مستطيلة مع فترة تركيز طويلة، مما يعني أنها قادرة على إعادة شحن المياه الجوفية بشكل فعال. خلال هطول الأمطار في نوفمبر ٢٠٢١، والتي جلبت ١٨,٧٨ ملم من الأمطار على مدار ٥ ساعات، استقبل وادي أبو عجاج معدلات تدفق قصوى بلغت ١١٩,٨ مترًا مكعبًا في الثانية وحجم جريان إجمالي قدره ٢,٣ مليون مترًا مكعبًا. كما أنتجت العاصفة غير المتوقعة في أغسطس ٢٠٢٤، بعمق هطول أمطار ٦٩,٧٢ ملم واستمرت ٤٦ ساعة، كمية هائلة من المياه الجارية ١٥,٦ مليون مترًا مكعبًا ، مع أقصى تدفق (٥١٥,٨ م٣ / ثانية) في وادي أبو عجاج. وتعتبر هذه العاصفة إحدى ظواهر التغير المناخي في مصر. تم اقتراح بعض التوصيات مثل إنشاء سدود احتجاز في مخارج وادي الحيتا والكمب وأم بويرات لتأخير تدفق المياه وتمكينها من التسرب التدريجي إلى المياه الجوفية وإنشاء سد تخزيني في منفذ وادي أبو عجاج لحماية المناطق الحضرية من مخاطر السيول الفجائية وتغذية طبقة المياه الجوفية الضحلة خلف السد.